Differential expression of mitochondrial energy metabolism profiles across the metaplasia–dysplasia–adenocarcinoma disease sequence in Barrett's oesophagus

J.J. Phelan [a], F. MacCarthy [b], R. Feighery [a], N.J. O'Farrell [a], N. Lynam-Lennon [a], B. Doyle [c], D. O'Toole [a], N. Ravi [a], J.V. Reynolds [a], J. O'Sullivan [a,*]

[a] Department of Surgery, Institute of Molecular Medicine, Trinity College Dublin, St. James's Hospital, Dublin, Ireland
[b] Department of Clinical Medicine, Institute of Molecular Medicine, Trinity College Dublin, St. James's Hospital, Dublin, Ireland
[c] Department of Pathology, St. James's Hospital, Dublin, Ireland

A B S T R A C T

Contemporary clinical management of Barrett's oesophagus has highlighted the lack of accurate predictive markers of disease progression to oesophageal cancer. This study aims to examine alterations in mitochondrial energy metabolism profiles across the entire disease progression sequence in Barrett's oesophagus. An *in-vitro* model was used to screen 84 genes associated with mitochondrial energy metabolism. Three energy metabolism genes (*ATP12A, COX4I2, COX8C*) were significantly altered across the *in-vitro* Barrett's disease sequence. *In-vivo* validations across the Barrett's sequence demonstrated differential expression of these genes. Tissue microarrays demonstrated significant alterations in both epithelial and stromal oxidative phosphorylation (ATP5B and Hsp60) and glycolytic (PKM2 and GAPDH) protein markers across the *in-vivo* Barrett's sequence. Levels of ATP5B in sequential follow up surveillance biopsy material segregated Barrett's non progressors and progressors to HGD and cancer. Utilising the Seahorse XF24 flux analyser, *in-vitro* Barrett's and adenocarcinoma cells exhibited altered levels of various oxidative parameters. We show for the first time that mitochondrial energy metabolism is differentially altered across the metaplasia–dysplasia–adenocarcinoma sequence and that oxidative phosphorylation profiles have predictive value in segregating Barrett's non progressors and progressors to adenocarcinoma.

Introduction

Barrett's oesophagus, defined pathologically as specialised intestinal metaplasia of the distal oesophagus, is a common preneoplastic lesion in the Western world [1]. Barrett's oesophagus arises from chronic gastroesophageal reflux disease (GORD) of acid and bile, and can progress to oesophageal adenocarcinoma (OAC) through low-grade dysplasia (LGD) and high-grade dysplasia (HGD) [2,3]. The measured annual risk of OAC in individuals with Barrett's metaplasia varies worldwide and is currently approximately 0.12% [2]. Barrett's oesophagus lacks any proven therapeutic strategy and despite numerous multimodality therapies, the prognosis for individuals with OAC still remains modest, with a commonly quoted 9–15% survival rate [4]. Some cancer centres, however, report survival in patients treated with curative intent to be approximately between 35% and 50% [5]. In addition, contemporary clinical management of Barrett's oesophagus through surveillance programs has highlighted the lack of accurate predictors of disease progression.

First reported by Otto Warburg in 1926, and thus coined the Warburg effect, cancer cells produce the majority of their ATP through aerobic glycolysis to support the extensive transformation, differentiation and aggressive proliferation of malignant cells [6]. These transformed cells convert the majority of incoming glucose to lactate rather than metabolising it through oxidative phosphorylation. Furthermore, despite aerobic glycolysis being more rapid at ATP production, it is far less efficient in terms of adenosine triphosphate (ATP) produced per molecule of glucose and therefore glucose uptake demands can function at abnormally high rates [6].

Studies investigating cancer metabolism have documented metabolic shifts from oxidative phosphorylation to aerobic glycolysis to generate energy. In human breast, gastric, squamous oesophageal and lung carcinomas, expression of mitochondrial and glycolytic protein markers varied significantly in carcinomas when

Abbreviations: ATP, Adenosine triphosphate; ATP5B, Adenosine triphosphate isoform 5B; OAC, Oesophageal adenocarcinoma; ECAR, Extracellular acidification rate; FCCP, Trifluorocarbonylcyanide phenylhydrazone; GAPDH, Glyceraldehyde 3-phosphate dehydrogenase; GORD, Gastroesophageal reflux disease; HGD, High-grade dysplasia; HSP60, Heat shock protein 60kD; LGD, Low-grade dysplasia; OCR, Oxygen consumption rate; PKM2, Pyruvate kinase isoform 2; TMAs, Tissue microarrays.

* Corresponding author. Tel.: +353 1 896 2149; fax: +353 145 46534.
E-mail address: osullij4@tcd.ie (J. O'Sullivan).

compared with paired normal tissues [7]. In the colonic mucosa of ulcerative colitis patients, mitochondrial complex activity is decreased between 50% and 60% compared with healthy controls [8]. This profile has also been documented in human kidney, liver and colonic carcinomas in tandem with increases in key glycolytic enzymes [9]. No study to date has investigated differential gene and protein expression associated with mitochondrial energy metabolism in Barrett's patients in such a sequential, retrospective and longitudinal manner.

The focus on the mitochondria as primary instigators of tumour progression is of great interest. It is speculated that the metabolic shift occurs as an adaption to defects in oxidative phosphorylation in the mitochondria since mitochondria lack DNA repair enzymes and are adjacent to cancer-causing free radicals [10]. The production of lactate during glycolysis may also facilitate tumour invasion and metastasis [11]. Other studies report that mitochondrial function is crucial for transformation in some tumour progression systems [12]. Moreover, a recent study has found that fidelity of the mitochondrial genome is increased in human colorectal cancer in conjunction with a shift in glucose metabolism from oxidative phosphorylation to glycolysis [13].

Despite innovative strategies in tumour detection and monitoring, for example, in fluorodeoxyglucose positron emission tomography imaging and glycolytic pathway inhibitors, a thorough understanding of the molecular mechanisms mediating tumour progression, particularly in Barrett's oesophagus and its progression to OAC is warranted [14]. Accordingly, more accurate predictors of disease progression should be validated, thus allowing early preneoplastic detection of such molecular mechanisms offering a greater insight into the risk of disease progression.

Therefore, the aim of this study was to examine mitochondrial energy metabolism gene and protein changes across the disease sequence *in-vitro* and *in-vivo* and to assess glucose metabolism across the disease sequence utilising two oxidative phosphorylation and two glycolytic protein markers. We have shown that genes associated with mitochondrial energy metabolism are differentially expressed across the metaplasia–dysplasia–OAC sequence both *in-vitro* and *in-vivo*. Furthermore, the Barrett's disease sequence exhibits significant alterations in the expression of oxidative phosphorylation and glycolytic proteins. Interestingly, levels of the oxidative phosphorylation protein ATP5B in sequential follow up material could significantly segregate Barrett's non progressors and progressors to cancer.

Material and methods

Metaplastic, dysplastic and adenocarcinogenic cell line models

QH (Barrett's), GO (dysplasia) and OE33 (OAC) cell lines, representing stages of the Barrett's disease sequence, were grown to 70% confluency in BEBM medium (OE33 in RPMI, 2 mM glutamine, 10% FBS, 1% penicillin-streptomycin L-glutamine) supplemented with BEBM SingleQuots (2 mL BPE, 0.5 mL insulin, 0.5 mL HC, 0.5 mL GA-1000, 0.5 mL retinoic acid, 0.5 mL transferring, 0.5 mL triiodothyronine, 0.5 mL adrenaline and 0.5 mL hEGF per 500 mL media). QH and GO cell lines were obtained from American Type Culture Collection (ATCC) (LGC Standards, Middlesex, UK). The OE33 cell line was sourced from the European Collection of Cell Cultures (Salisbury, UK). Cell RNA extractions were subsequently performed using RNeasy Mini Kit (Qiagen) following manufacturer's instructions. RNA content and quality was quantified and assayed respectively and RNA reverse transcribed using the RT^2 PCR array first strand kit (SABiosciences).

Screening via qRT-PCR microarray analysis

A catalogued human mitochondrial energy metabolism PCR gene microarray (Qiagen) was used to simultaneously quantify the expression of 84 mitochondrial genes across the *in-vitro* sequence using *B2M* as the endogenous control gene. PCR was performed using the RT^2 Realtime SYBR Green PCR mix (SABiosciences) following manufacturer's instructions on a 7900HT Fast Realtime PCR Light-Cycler System (Applied Biosystems). Data were analysed utilising the $2^{-\Delta\Delta Ct}$ method. First, threshold cycle (Ct) values were converted to 2^{-Ct} in order to be proportional to the amount of transcripts in all samples. Next, $2^{-\Delta Ct}$ values were calculated by normalising the data to a housekeeping gene, beta-2-microglobulin (B2M), as follows: $2^{-\Delta Ct} = 2^{-Ct}$ (sample) / 2^{-Ct} (B2M). In order to compare the data between cell line models, $2^{-\Delta\Delta Ct}$ values were calculated by normalising the experimental data by reference data. For example, data from the calibrator QH cell line was normalised to the GO cell line as follows: $2^{-\Delta\Delta Ct} = 2^{-\Delta Ct}$ (QH) / $2^{-\Delta Ct}$ (GO). Differentially expressed genes were defined as those that changed by >4-fold.

In-vitro validation of gene targets

Cell lines were cultured and RNA extracted as described above. RNA was reverse transcribed using Bioscript enzyme (Bioline). Gene primer probes for *COX8C*, *COX4I2*, *ATP12A* and *18S* (Applied Biosystems) were purchased and realtime PCR was performed using Taqman mastermix (Applied Biosystems). Data were analysed utilising the $2^{-\Delta\Delta Ct}$ method.

In-vivo validation of gene targets

The expression of these three genes was analysed in independent groups of tissues across the Barrett's sequence. Ethical approval to conduct all aspects of this work was granted by the Adelaide and Meath Hospital (AMNCH), Tallaght, Dublin (REC 200110405). All cases were prospectively recruited at our national referral centre for upper GI malignancy. Written informed consent was obtained in accordance with local institutional ethical guidelines. All patients attending with histologically confirmed Barrett's oesophagus or OAC arising in Barrett's were considered for inclusion. Patients with a prior history of treated OAC (including *in situ* carcinoma post endomucosal resection), other malignancy of any type, ablative therapy (radiofrequency ablation, argon plasma coagulation, cryoablation) were excluded.

Endoscopic examination consisting of white light and chromoendoscopy (FICE (Fujinon) or NBI (Olympus)) was performed in all cases (DOT, NR and FMC). The Barrett's segment was assessed and measured as per the Prague classification system. Suspicious sites were biopsied using large capacity forceps in the first instance, with mapping biopsies performed thereafter as per international guidelines. Matched squamous samples were taken at least 5 cm superior to the proximal border of Barrett's mucosa.

Normal control samples, demonstrating normal squamous mucosa, were taken from individuals attending for upper GI endoscopy without symptoms to suggest GORD or other inflammatory aetiology. Cancer samples were taken from individuals undergoing assessment for a new diagnosis of OAC arising in a setting of Barrett's oesophagus. All samples were placed in RNAlater at the time of endoscopy. Barrett's tissue was characterised by assessing the expression of columnar epithelium molecular markers, cytokeratin 8 and villin by RTPCR.

Patient material was homogenised using a Tissue-Lyser (Qiagen) for 5 min at a frequency of 25 pulses per second, RNA extracted, reverse transcribed (Bioline), RNA quantified (NanoDrop, Technologies, Wilmington, DE, USA) and sample quality assessed using the RNA Nano 6000 kit (Agilent Technologies, Santa Clara, CA, USA). Realtime PCR was performed and all genes validated similarly across the diseased Barrett's sequence *in-vivo* utilising normal squamous ($n = 10$), metaplasia ($n = 34$), LGD ($n = 13$), HGD ($n = 12$) and OAC ($n = 8$) cases.

ATP5B, Hsp60, PKM2 and GAPDH immunohistochemistry analysis using tissue microarrays

Immunohistochemistry was performed utilising normal squamous ($n = 17$), oesophagitis (41), metaplasia ($n = 66$), LGD ($n = 32$), HGD ($n = 12$) and OAC ($n = 20$) cases. The areas of interest on the diagnostic biopsy blocks were marked by a pathologist (BD) and 0.6 mm cores were taken from the blocks and tissue microarrays (TMAs) were constructed. Immunohistochemistry was performed using the TMAs utilising the Vectastain Kit (Elite) as per manufacturer's instructions. All sections were processed and stained on the same day. Endogenous peroxidases were quenched in 3% hydrogen peroxide (in methanol) for 30 min and slides blocked for 30 min. Primary oxidative phosphorylation antibodies included an anti-ATP5B IgG (Santa Cruz Biotechnology) and an anti-Hsp60 IgG (Abcam) diluted 1:1000 and 1:400 in PBS respectively. Primary glycolytic antibodies used were an anti-PKM2 IgG (Abgent) and an anti-GAPDH IgG (AbDserotec Division of MorphoSys) both diluted 1:100 in PBS. Slides were incubated with primary antibody for 1 hour, biotinylated antibody for 30 minutes, incubated with avidin-biotin complex for 30 minutes and DAB substrate for 2–15 minutes. DAB was rinsed off slides upon colour development and haematoxylin added for 30 seconds. Lastly, slides were dehydrated and mounted using DPX. Slides were scanned (Aperio Scanscope XT digital scanner, University College Dublin) and immunoreactivity was assessed digitally under 40× magnification in a semi-quantitative manner for each protein by observers (JP and JOS) who were blinded to the pathological and clinical diagnosis of all patients in the study. For each protein, both epithelial and stromal cells were evaluated for both percentage positivity and intensity of cytoplasmic staining. Intensity was graded as 0 (negative), 1 (weak), 2 (moderate) and 3 (strong) and positivity was categorised as 0%, 10%, 25%, 50%, 75%, 90% or 100%.

Characterising the metabolic plasticity of Barrett's and adenocarcinoma cell lines utilising the Seahorse XF24 analyser

Oxygen consumption rate (OCR) and extracellular acidification rate (ECAR), reflecting oxidative phosphorylation and glycolysis respectively, were measured before and subsequent to treatment with oligomycin (2 μg·mL^{-1}, Seahorse Biosciences), trifluorocarbonylcyanide phenylhydrazone (FCCP) (5 μM, Seahorse Biosciences) and antimycin-A (2 μM, Seahorse Biosciences) using the Seahorse XF24 analyser (Seahorse Biosciences). QH and OE33 cells were seeded at 20,000 cells per well in a 24-well cell culture XF microplate (Seahorse Biosciences) and allowed to adhere for 24 hours. Cells were rinsed with assay medium (unbuffered DMEM supplemented with 10 mM glucose and 20 mM sodium pyruvate, pH 7.4) before incubation with assay medium for 1 hour at 37 °C in a non-CO_2 incubator. Four baseline OCR and ECAR measurements were obtained over 28 minutes before injection of specific metabolic inhibitors. Three OCR and ECAR measurements were obtained over 15 minutes following injection with oligomycin, FCCP and antimycin-A. Percentage ATP synthesis was calculated by subtracting the OCR post oligomycin injection from baseline OCR prior to oligomycin addition and expressing residual OCR as a percentage of baseline OCR. Proton leak was calculated by subtracting percentage OCR versus baseline post antimycin-A addition from percentage ATP synthesis. The experiment was repeated five times ($n = 5$) with adequate technical replicates. All measurements were normalised to cell number using the crystal violet assay.

Statistical analysis

Data were analysed using Graph Pad Prism (Graph Pad Prism, San Diego, CA, USA) and SPSS (PASW [Predictive Analytics Software] version 18) (IBM, Armonk, New York, USA) software. qRT-PCR data were normalised using the $2^{-\Delta\Delta Ct}$ method and statistically analysed (Kruskal–Wallis, Mann–Whitney *U*). qRT-PCR target genes were statistically analysed (Wilcoxon sign rank) in matched patient samples to explore if observed gene expression changes were an effect seen in the Barrett's tissue compared with the surrounding mucosa. Immunohistochemical differences between individual histological groups (Mann–Whitney *U*) and across the Barrett's sequence (Kruskal–Wallis) were statistically analysed. Categorical differences between Barrett's metaplasia progressors and non-progressors was analysed using chi-square tests, and Mann–Whitney *U* tests were used to determine differences between percentage positivity. Student's unpaired *t*-test was utilised to compare Seahorse metabolics in two groups of normally distributed independent groups. Differences of $P < 0.05$ (*), $P < 0.01$ (**) and $P < 0.001$ (***) were considered statistically significant.

Results

In-vitro *screening using human PCR gene microarrays*

To analyse expression of human 84 mitochondrial energy metabolism genes across the disease sequence *in-vitro*, fold expression of all target genes was normalised relative to the Barrett's metaplastic cell line model, QH. The cut-off for differential gene expression was defined by either a relative fourfold upregulation or fourfold downregulation. Three of the 84 mitochondrial energy metabolism gene targets (*ATP12A*, *COX4I2* and *COX8*) were differentially expressed across the metaplastic–dysplastic–OAC cell line sequence. These three gene targets identified were subsequently validated *in-vitro* and *in-vivo* using patient samples.

Figure 1 shows the *in-vitro* PCR gene microarray screen between the Barrett's, dysplastic and OAC cells and the subsequent *in-vitro* validation of the three mitochondrial energy metabolism gene targets. Using a fourfold cut-off, six gene targets were found to be differentially expressed between QH and GO cells (Fig. 1A). Using a fourfold cut-off, two gene targets were found to be differentially expressed between GO and OE33 cells (Fig. 1B). Using a fourfold cut-off, six gene targets were found to be differentially expressed between the QH and OE33 cells (Fig. 1C). Table 1 summarises the relative expression of all 84 genes screened between QH and OE33 cell lines (see Supplementary material Table S1 for additional PCR microarray screen results between GO and OE33 and between GO and QH cells). *ATP12A* ($P < 0.05$) expression significantly decreased across the Barrett's sequence (Fig. 1D). *COX4I2* expression decreased; however, this was not statistically significant (Fig. 1E). *COX8C* ($P < 0.05$) expression significantly increased between Barrett's and dysplastic cell lines ($P < 0.05$) but subsequently decreased between dysplastic and OAC cell lines; however, this was not statistically significant (Fig. 1F).

Table 1
Energy metabolism gene microarray screen between QH and OE33 cell lines.

Gene	Expression*	Gene	Expression*	Gene	Expression*
ATP4A	6.32	*COX6B1*	2.57	*NDUFB8*	−1.18
ATP4B	3.67	*COX6B2*	1.25	*NDUFB9*	1.34
ATP5A1	8.05	*COX6C*	1.33	*NDUFC1*	1.1
ATP5B	−1.07	*COX7A2*	5.17	*NDUFC2*	−1.02
ATP5C1	1.04	*COX7A2L*	1.13	*NDUFS1*	1.53
ATP5F1	1.33	*COX7B*	−1.06	*NDUFS2*	1.22
ATP5G1	1.28	*COX8A*	1.49	*NDUFS3*	−2.01
ATP5G2	−1.69	*COX8C*	1.49	*NDUFS4*	1.26
ATP5G3	−1.40	*CYC1*	6.84	*NDUFS5*	−1.45
ATP5H	−2.00	*LHPP*	1.13	*NDUFS6*	−1.55
ATP5I	−1.03	*NDUFA1*	1.38	*NDUFS7*	1.93
ATP5J	−1.59	*NDUFA10*	−1.04	*NDUFS8*	−1.59
ATP5J2	−1.70	*NDUFA11*	1.09	*NDUFV1*	1.22
ATP5L	3.83	*NDUFA2*	−1.48	*NDUFV2*	1.57
ATP5O	−1.11	*NDUFA3*	−1.37	*NDUFV3*	−1.71
ATP6V0A2	−1.44	*NDUFA4*	1.1	*OXA1L*	1.03
ATP6V0D2	2.21	*NDUFA5*	1.04	*PPA1*	−1.24
ATP6V1C2	1.54	*NDUFA6*	−1.92	*PPA2*	2.17
ATP6V1E2	2.21	*NDUFA7*	1.53	*SDHA*	−1.1
ATP6V1G3	1.66	*NDUFA8*	−1.6	*SDHB*	1.94
ATP12A	6.32	*NDUFAB1*	−1.3	*SDHC*	−1.78
BCS1L	5.92	*NDUFB10*	1.52	*SDHD*	−2.30
COX4I1	1.04	*NDUFB2*	3.98	*UQCR11*	−1.67
COX4I2	−1.21	*NDUFB3*	−1.42	*UQCRC1*	−1.27
COX5A	9.84	*NDUFB4*	−1.04	*UQCRC2*	−2.13
COX5B	1.16	*NDUFB5*	1.15	*UQCRFS1*	1.8
COX6A1	1.22	*NDUFB6*	1.01	*UQCRH*	1.02
COX6A2	1.06	*NDUFB7*	−1.33	*UQCRQ*	−1.88

B2M, endogenous control gene.
* Relative expression (e.g. expression of *ATP4A* is 6.32 times greater in OE33 than QH cells).

In-vivo *validation of gene targets*

Figure 2 illustrates mitochondrial energy metabolism gene expression of the three gene targets across the disease sequence in diseased and matched normal adjacent tissue samples. *ATP12A* (Fig. 2A) ($P < 0.001$), *COX4I2* (Fig. 2C) ($P < 0.01$) and *COX8C* (Fig. 2E) ($P < 0.05$) were found to be differentially expressed across the Barrett's sequence. Field effect changes in gene expression of these targets in diseased versus matched normal adjacent biopsies were examined. *ATP12A* (Fig. 2B) ($P < 0.001$), *COX4I2* (Fig. 2D) ($P < 0.01$) and *COX8C* (Fig. 2F) ($P < 0.01$) were found to be differentially expressed across the Barrett's disease sequence suggesting this effect was specific to the pathological diseased tissue (Barrett's, LGD, HGD and OAC) compared with the matched surrounding matched mucosa.

Oxidative phosphorylation and glycolytic activity across Barrett's sequence

To assess oxidative phosphorylation at the protein level, levels of ATP5B and HSP60 were assessed as no reliable antibodies to ATP12A, COX4I2 and COX8C have yet been developed. Even though ATP5A is a direct component of the electron transport chain and thus an effective determinant of oxidative phosphorylation, HSP60 is increasingly being used as a surrogate marker for mitochondrial function and for the assessment of oxidative mitochondrial metabolism due to its role as an active mitochondrial chaperone. Figure 3 shows immunohistochemical expression of these oxidative phosphorylation protein biomarkers across the metaplasia–dysplasia–OAC disease sequence. Figure 3A and 3B shows representative images of ATP5B expression in oesophagitis and OAC tissue respectively. Figure 3C and 3D shows representative images of Hsp60 expression in oesophagitis and HGD tissue respectively. Epithelial ATP5B positivity across the Barrett's disease sequence was increased significantly (Fig. 3E) ($P = 0.0003$). Moreover, epithelial Hsp60 positivity

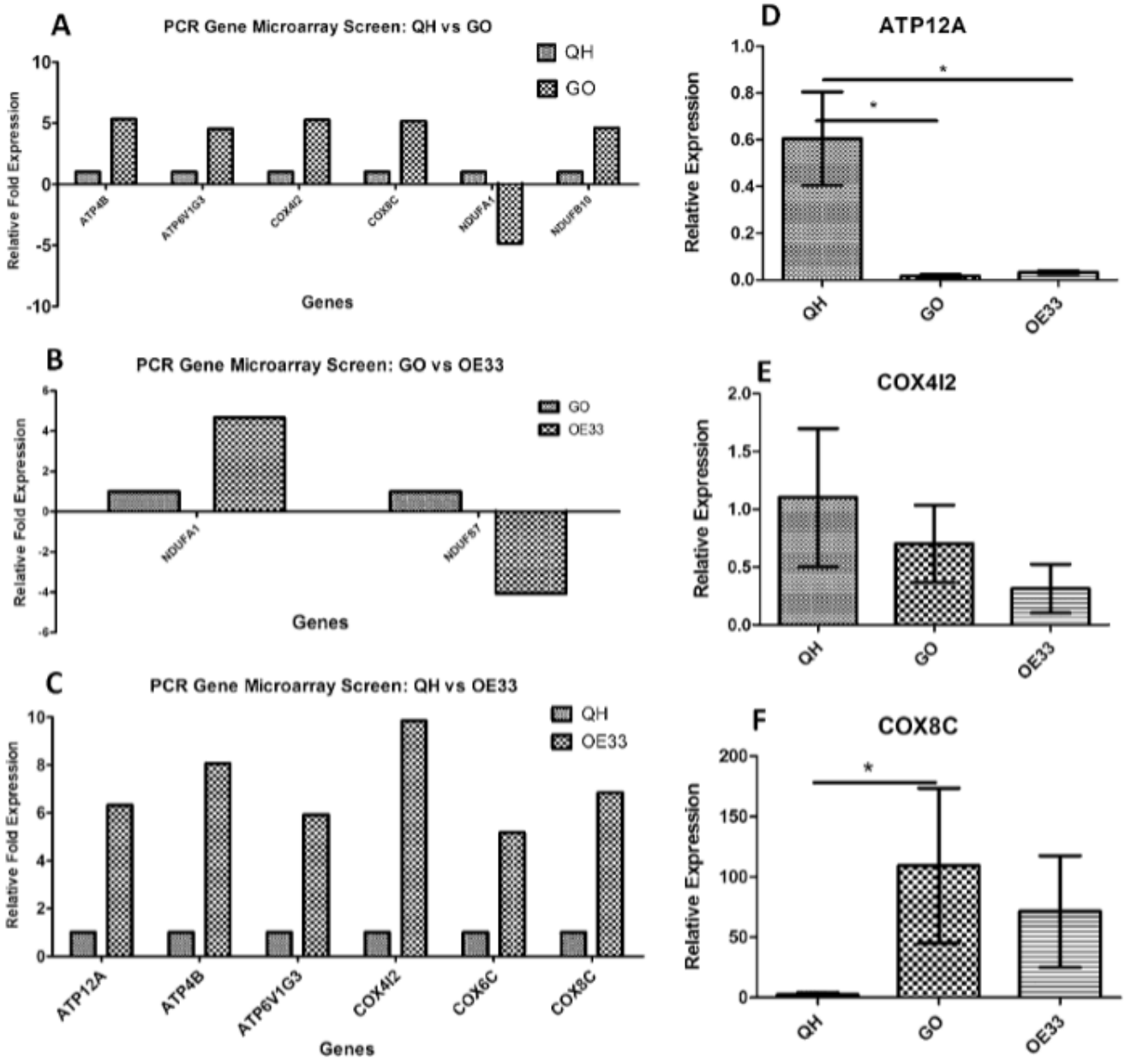

Fig. 1. Human PCR gene microarray screen and *in-vitro* validation of mitochondrial energy metabolism gene targets found to be differentially expressed across the Barrett's cell lines. (A) Using a fourfold cut-off, six gene targets were found to be differentially expressed between the Barrett's (QH) and dysplastic (GO) cell lines. (B) Using a four-fold cut-off, two gene targets were found to be differentially expressed between the dysplastic (GO) and adenocarcinoma (OE33) cell lines. (C) Using a fourfold cut-off, six gene targets were found to be differentially expressed between the Barrett's (QH) and adenocarcinoma (OE33) cell lines. (D) ATP12A ($P < 0.05$), (E) COX4I2 ($P > 0.05$) and (F) COX8C ($P < 0.05$) were found to be differentially expressed between the *in-vitro* Barrett's cell lines (unpaired *t*-test) (Bonferroni post-hoc test). One-way ANOVA was used to investigate differences across the *in-vitro* Barrett's sequence for ATP12A ($P < 0.05$), COX4I2 ($P > 0.05$) and COX8C ($P = 0.072$). Bars denote mean ± SEM.

across the Barrett's disease sequence was increased significantly (Fig. 3F) ($P < 0.0001$). Interestingly, no significant changes in the levels of both oxidative phosphorylation markers ATP5B and HSP60 were detected in stromal tissue across the Barrett's sequence. Moreover, Figure 3G and 3H respectively shows that epithelial expression levels of ATP5B ($P < 0.0001$) and HSP60 ($P < 0.05$) were significantly altered across the Barrett's disease sequence in matched normal adjacent.

Figure 4 illustrates epithelial and stromal tissue expression of the glycolytic protein markers, PKM2 and GAPDH, across the metaplastic–dysplastic–OAC disease sequence. Figure 4A and 4B shows representative images of epithelial PKM2 expression in oesophagitis and HGD tissue respectively. Figure 4C and 4D shows representative images of epithelial GAPDH expression in Barrett's and OAC tissue respectively. Epithelial PKM2 positivity across the Barrett's disease sequence was shown to increase significantly (Fig. 4E) ($P = 0.0003$). Epithelial GAPDH positivity also increased significantly across the Barrett's disease sequence (Fig. 4F) ($P = 0.0002$). In contrast to the markers of oxidative phosphorylation in the stromal compartment, stromal tissue expression of the glycolytic protein

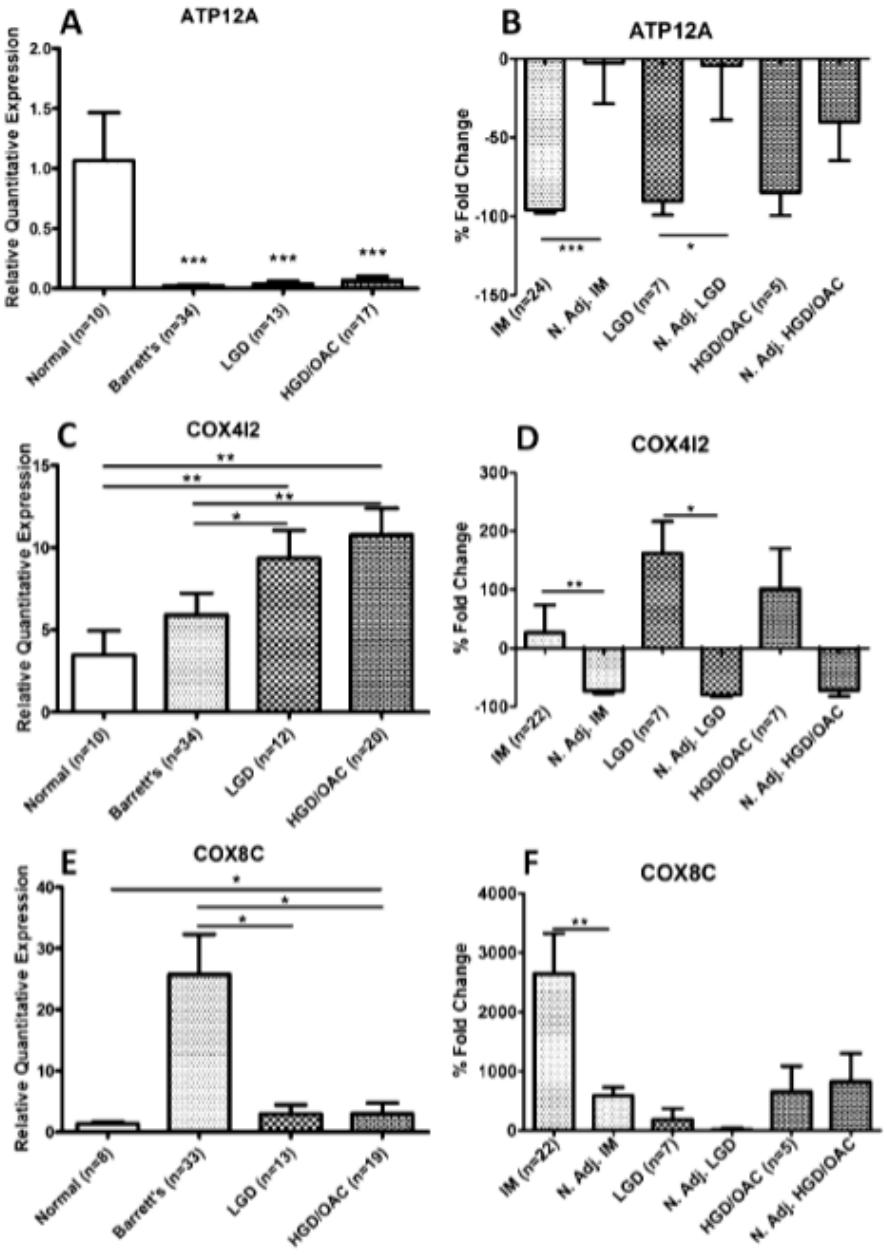

Fig. 2. Mitochondrial energy metabolism gene expression across the disease sequence in diseased (A, C and E) versus matched normal adjacent (B, D and F) *in-vivo* samples. (A) ATP12A ($P < 0.001$), (C) COX4I2 ($P < 0.01$) and (E) COX8C ($P < 0.05$) were found to be differentially expressed across the Barrett's disease sequence (Kruskal–Wallis test, Mann–Whitney *U*). (B) ATP12A ($P < 0.001$), (D) COX4I2 ($P < 0.01$) and (F) COX8C ($P < 0.01$) were found to be differentially expressed across the Barrett's disease sequence (Wilcoxon sign rank). Bars denote mean ± SEM.

markers, PKM2 (Fig. 4G) ($P = 0.03$) and GAPDH (Fig. 4H) ($P = 0.0007$), decreased significantly across the metaplastic–dysplastic–OAC disease sequence.

In addition to analysing the expression of the protein markers ATP5B and HSP60 in independent groups of tissue across the Barrett's sequence, we assessed their expression in sequential longitudinal material from Barrett's non progressors and progressors to investigate a potential predictive biomarker of OAC. Focusing on patients with a primary diagnosis of intestinal metaplasia on first surveillance endoscopy, Barrett's non-progressors ($n = 15$) and progressors ($n = 11$) were separated with the primary end-point being progression to OAC. The median age of patients with intestinal metaplasia was 58 years and there was a 3.3-fold male predominance. There was no significant difference in age between progressors and non-progressors ($P = 0.6404$). Median time of progression to cancer was 2.6 years. TNM staging for progressors was as follows: 20% $T_1N_0M_0$, 20% $T_3N_1M_X$, 20% $T_{IS}N_0M_0$, 10% $T_{IS}N_0M_0$, 10% $T_3N_0M_0$, 10% $T_3N_1M_0$ and 10% $T_3N_1M_1$. The non-progressor group was followed for a median of 5.4 years and had no evidence of conversion to HGD and/or OAC. Figure 5 illustrates the longitudinal tissue microarray expression of the metabolic biomarkers ATP5B, HSP60, PKM2 and GAPDH between Barrett's patients who did and did not progress using initial first-time surveillance biopsies from these patients. Interestingly, there was a significant increase in mean

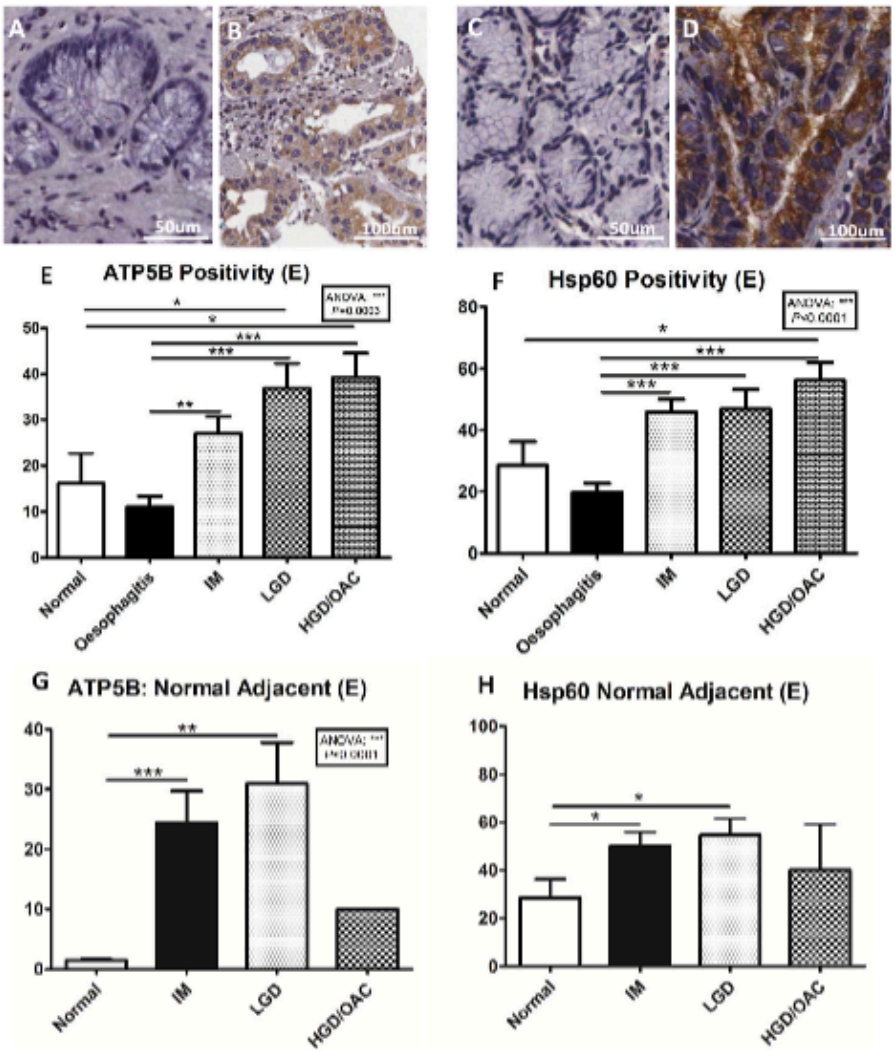

Fig. 3. Epithelial immunohistochemical tissue expression of the oxidative phosphorylation protein biomarkers, ATP5B (A, B, E and G) and Hsp60 (C, D, F and H), across the metaplasia–dysplasia–adenocarcinoma disease sequence. (A) Tissue section from an oesophagitis patient negative for levels of epithelial ATP5B staining. (B) Tissue section from an OAC patient positive for levels of ATP5B staining in epithelium. (C) Tissue section from an oesophagitis patient with negative levels of epithelial Hsp60 staining. (D) Tissue section from a HGD patient exhibiting positive levels of Hsp60 staining in epithelium. (E) Epithelial ATP5B positivity across the Barrett's disease sequence was shown to increase significantly ($P < 0.001$, Mann–Whitney *U*) (ANOVA; $P = 0.0003$). (F) Epithelial Hsp60 positivity across the Barrett's disease sequence increased significantly ($P < 0.001$, Mann–Whitney U) (ANOVA; $P < 0.0001$). (G) Epithelial ATP5B positivity early across the Barrett's disease sequence in matched normal adjacent tissue was shown to increase significantly ($P < 0.0001$, Mann–Whitney *U*) (ANOVA; $P < 0.0001$). (H) Epithelial Hsp60 positivity early across the Barrett's disease sequence in matched normal adjacent tissue increased significantly ($P < 0.05$, Mann–Whitney *U*).

percentage positivity of stromal cytoplasmic ATP5B in Barrett's patients who prospectively progressed to OAC (Fig. 5A) ($P < 0.01$). This predictive protein was specific to ATP5B and not the other metabolic markers (Fig. 5B–D).

Characterisation of oxidative metabolic plasticity in the in-vitro *Barrett's sequence*

As ATP5B, the marker of oxidative phosphorylation, was predictive in segregating Barrett's non progressors and progressors, we examined how metaplastic and OAC cells would behave when challenged with mitochondrial inhibitors known to alter metabolic reprogramming. Figure 6 illustrates different metabolic parameters examined subsequent to challenging QH and OE33 cell lines with oligomycin, FCCP and antimycin-A using the Seahorse XF24 flux analyser. Figure 6A–F illustrates relative mitochondrial respiration in QH and OE33s cells, ATP synthesis, maximal respiratory capacity, non electron transport chain respiration and proton leak between the QH and OE33 cell lines, respectively. Approximately 80% of total OCR accounted for mitochondrial respiration in the QH cell line (Fig. 6A) and 64.7% of total OCR accounted for mitochondrial respiration in the OE33 cell line (Fig. 6B). Levels of oxygen consumed by the electron transport chain in both cell lines was significantly higher versus oxygen consumed for non electron transport chain purposes (Fig. 6A–B) ($P < 0.001$). QH cells (63%) exhibited higher levels of ATP synthesis compared with the OE33 (50.6%) cells (Fig. 6C) ($P < 0.05$). Upon mitochondrial uncoupling with FCCP, OE33 cells exhibited a significantly greater spare respiratory capacity of 33% versus QH cells (Fig. 6D) ($P < 0.01$). OE33 cells demonstrated 15.2% higher levels of OCR, attributed to non electron transport chain processes, compared with QH cells (Fig. 6E) ($P < 0.05$).

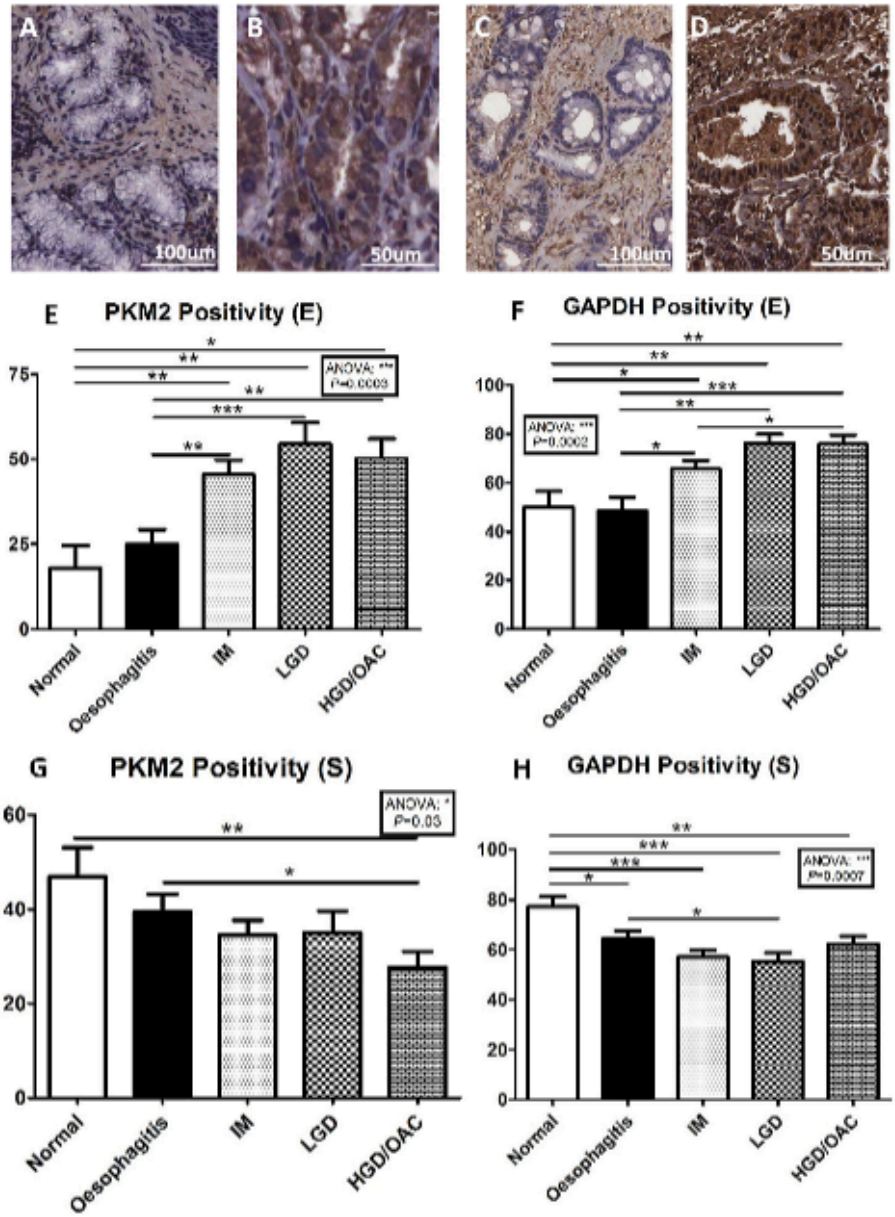

Fig. 4. Epithelial and stromal immunohistochemical tissue expression of the glycolytic protein markers, PKM2 (A, B, E and G) and GAPDH (C, D, F, H), across the metaplasia–dysplasia–adenocarcinoma disease sequence. (A) Tissue section from an oesophagitis patient negative for levels of epithelial PKM2 staining. (B) Tissue section from a HGD patient positive for levels of PKM2 staining in epithelium. (C) Tissue section from a Barrett's oesophagus patient exhibiting minimal baseline levels of epithelial GAPDH staining. (D) Tissue section from an OAC patient exhibiting strong positive levels of GAPDH staining in epithelium. (E) Epithelial PKM2 positivity across the Barrett's disease sequence was shown to increase significantly ($P < 0.001$, Mann–Whitney U) (ANOVA; $P = 0.0003$). (F) Epithelial GAPDH positivity increased significantly across the Barrett's disease sequence ($P < 0.001$, Mann–Whitney U) (ANOVA; $P = 0.0002$). (G) Stromal PKM2 positivity across the Barrett's disease sequence was shown to decrease significantly ($P < 0.01$, Mann–Whitney U) (ANOVA; $P = 0.03$). (H) Stromal GAPDH positivity decreased significantly across the Barrett's disease sequence ($P < 0.001$, Mann–Whitney U) (ANOVA; $P = 0.0007$).

Discussion

Understanding the underlying molecular mechanisms that support the progression of Barrett's oesophagus to cancer would significantly affect the clinical management of these patients. We have shown for the first time that mitochondrial energy metabolism is altered across the normal–metaplasia–dysplasia–OAC sequence of events in Barrett's oesophagus and these early changes in metabolic alterations, specifically oxidative phosphorylation, are associated with an increased risk of disease progression from Barrett's metaplasia to OAC.

In this study, a human PCR gene microarray identified three genes associated with mitochondrial energy metabolism differentially expressed between Barrett's and OAC cells. Few studies have associated *COX4I2*, *COX8C*, and *ATP12A* with cancer progression and their role in energy metabolism. We have shown a significant increase in *COX8C* expression in Barrett's patients compared with normal squamous tissues. Interestingly, the increase in *COX8C* expression in Barrett's tissue was subsequently followed by a significant decrease in *COX8C* expression in LGD and HGD/cancer tissue. This increase in *COX8C* expression was specific to Barrett's tissue compared with matched surrounding mucosa. No studies to date have reported a role for

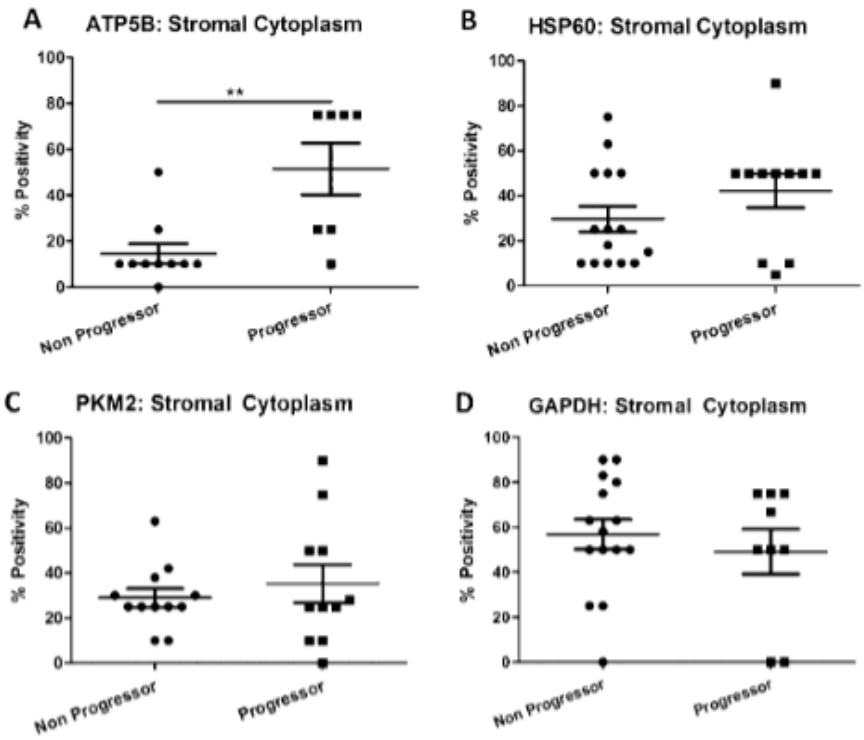

Fig. 5. Longitudinal immunohistochemical assessment of mean ATP5B (A), HSP60 (B), PKM2 (C) and GAPDH (D) tissue microarray expression in Barrett's non-progressors and progressors to OAC. (A) Barrett's patients who prospectively progressed to OAC exhibited significantly increased levels of ATP5B ($P = 0.007$, Mann–Whitney *U*). (B) HSP60 expression was not significantly different between Barrett's non-progressors and progressors to OAC ($P > 0.05$, Mann–Whitney *U*). (C) PKM2 levels were not significantly different between Barrett's non-progressors and progressors to OAC ($P > 0.05$, Mann–Whitney *U*). (D) GAPDH expression was not significantly different between Barrett's non-progressors and progressors to OAC ($P > 0.05$, Mann–Whitney *U*). For ATP5B and GAPDH, seven and nine progressors were deemed scorable respectively. Bars denote mean ± SEM.

COX8C in tumourigenesis, therefore, we hypothesise that *COX8C* may play an important role in Barrett's patients by increasing basal oxidative phosphorylation levels, altering energy metabolism and subsequently promoting neoplastic progression.

We have also shown *in-vivo* a significant increase in *COX4I2* expression across the Barrett's sequence. *COX8C* and *COX4I2* pertain to the one protein complex and both have different expression patterns – *COX8C* increases and subsequently decreases while *COX4I2* increases and maintains its expression pattern. Interestingly, both complex IV genes are upregulated despite a significant downregulation in a subunit of their downstream associate complex, ATP synthase. This downregulation of *ATP12A* was also shown to be specific to Barrett's tissue compared with the matched surrounding mucosa.

COX4I2 and *ATP12A* have been ascribed to few pathologies. A single base mutation in the *ATP12A* subunit results in complex V deficiency [15]. Immunological ATP12A expression in normal and benign prostate hyperplasia and cancerous prostate tissue have been shown to be altered in luminal cells of the glandular epithelium [16]. More recently, in a study proposing a protective role for decreased ATP levels analysing the function of lung-specific *COX4I2 in-vitro* and in *COX4I2*-knockout mice *in-vivo*, it was found that cytochrome *c* oxidase activity and ATP levels were significantly reduced in knockout mice [17]. In addition, decreased oxidative phosphorylation in cancer development is commonly associated with a parallel increase in glycolysis [18–22]. This decrease in oxidative phosphorylation is frequently linked with defects in complex I and III, for example, in renal, leukaemia and fibroblast cell lines [18,20,22]. One possible explanation for the dysregulation of these three genes is in the microenvironment they reside. Mitochondrial DNA is highly prone to oxidative damage as it is situated on the inner mitochondrial membrane [23]. Moreover, it is in close proximity to the electron transport chain and the levels of oxidised bases are estimated to be two to three times greater than nuclear DNA [23]. The increased oxidative microenvironment demonstrated in this study may strengthen this hypothesis in Barrett's oesophagus.

Next, we investigated the expression of different oxidative phosphorylation and glycolytic proteins across the Barrett's sequence and investigated if the metabolic phenotype at the protein level reflected these metabolic profiles seen at the gene level and investigated if a metabolic marker could segregate Barrett's non-progressors and progressors to cancer using established markers of oxidative phosphorylation (ATP5B and HSP60) and glycolysis (PKM2 and GAPDH) [13,24,25].

We have shown that both epithelial ATP5B and HSP60 positivity significantly increased across the Barrett's sequence, consistent with a metabolic shift in glucose metabolism to a more actively oxidative metabolic level. Moreover, the expression levels of ATP5B and HSP60 were significantly altered between Barrett's diseased tissue and the matched surrounding mucosa. This increase in oxidative phosphorylation is analogous to *COX4I2* and *COX8C* discussed above. One recent study showed a similar trend in glucose metabolism whereby human breast tumours demonstrated increased epithelial enzymatic activity in various complexes [26]. To recall, HSP60 positivity significantly increased across the Barrett's sequence. HSP60 expression has been previously shown to be increased in various cancer types [27–29]. This increase in oxidative phosphorylation complex IV genes and associated proteins highlighted may be a com-

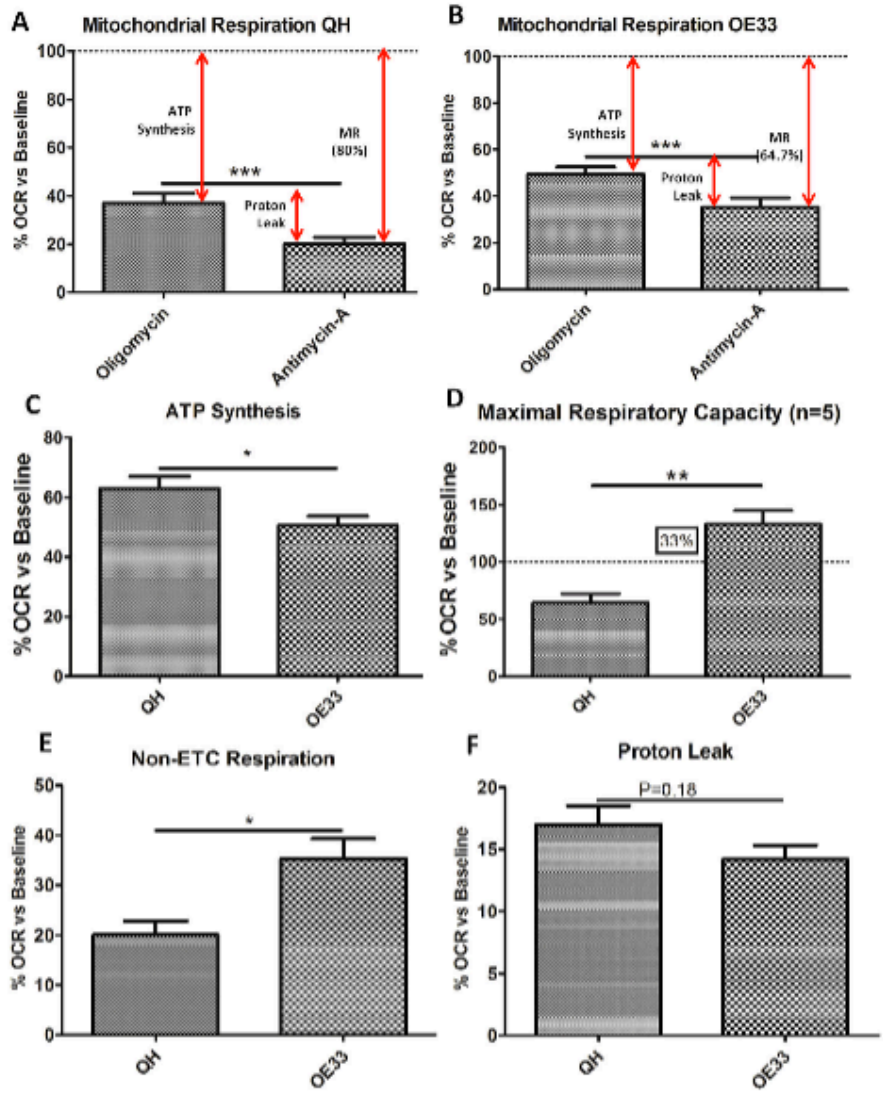

Fig. 6. Seahorse assessment of mitochondrial respiration (A–B), ATP synthesis (C), maximal respiratory capacity (D), non electron transport respiration (E) and proton leak (F) between the Barrett's (QH) and adenocarcinoma (OE33) *in-vitro* cell lines. (A) Measurement of mitochondrial respiration (37%) and proton leak (17%) in the Barrett's metaplasia cell line, QH ($P < 0.001$). (B) Measurement of mitochondrial respiration (49.4%) and proton leak (14.2%) in the oesophageal adenocarcinoma cell line, OE33 ($P < 0.001$). (C) Graph shows the percentage of oxygen consumption versus baseline reflecting ATP production attributed to ATP synthase after ATP synthase inhibition via oligomycin. QH cells (63%) utilise significantly higher levels of oxygen for oxidative phosphorylation ($P < 0.05$) in contrast to OE33 cells (50.6%). (D) Graph illustrates the percentage of oxygen consumption versus baseline upon mitochondrial uncoupling via trifluorocarbonylcyanide phenylhydrazone (FCCP). OE33 cells exhibited a greater spare respiratory capacity (33%) versus the QH cell line ($P < 0.01$). (E) The OE33 cell line (35.2%) demonstrated significantly higher non-electron transport chain respiration levels compared with the QH cell line (20%) ($P < 0.05$). (F) The Barrett's QH cell line (17%) exhibited higher cells of proton leak across the inner mitochondrial membrane versus the adenocarcinoma OE33 cell line (14.2%) ($P = 0.18$). Bars denote mean ± SEM.

pensatory mechanism to counteract the significant downregulation of complex IV's main downstream protein complex, complex V, namely attributed to *ATP12A* as this loss can lead to complete mitochondrial dysfunction [15]. Therefore, we hypothesise that cancer cells may act as 'metabolic parasites', secreting hydrogen peroxide into the local microenvironment, inducing oxidative stress in normal host cells resulting in autophagy, mitophagy and aerobic glycolysis. As a result, high-energy glycolytic nutrients such as ketones, L-lactate and glutamine may fuel the anabolic growth of tumour cells through oxidative phosphorylation.

The epithelial expression of both glycolytic biomarkers, PKM2 and GAPDH, were significantly increased across the Barrett's sequence and concur with an elevation in epithelial glycolysis, a common entity shown in other cancers [13,30,31]. PKM2 is more abundant during aerobic glycolysis in many tumour types, including the Barrett's sequence in non-sequential tissue [32]. Interestingly, in contrast to the increased epithelial expression of both glycolytic makers, the expression of these markers is significantly decreased in matched stromal tissue. However, the proliferation status of the epithelium may in part exacerbate the degree of aerobic glycolysis. Interestingly, our longitudinal analysis demonstrates that Barrett's patients with increased levels of the oxidative phosphorylation marker ATP5B are more likely to progress to OAC. This novel finding indicates a crucial and pivotal role for oxidative phosphorylation in OAC progression in the Barrett's disease sequence. Increased levels of ATP5B, and thus oxidative phosphorylation, are fuelled by the greater availability of high-energy nutrients through increased glycolysis. As a result, the subsequent oxidative state may

make local tissue more amenable to the anabolic growth of tumour cells, tumour differentiation and progression. Subsequent validation of ATP5B in different patient cohorts from different clinical institutions would potentially strengthen the applicability of this marker in the clinical setting as this assessment could be undertaken efficiently on formalin fixed paraffin embedded tissue.

It is evident from this study that oxidative phosphorylation at both the gene and protein level play a vital role in exacerbating disease progression in Barrett's oesophagus. It was necessary, therefore, to decipher elements of oxidative phosphorylation, specifically the complexes of the electron transport chain that play an important role. Using the Seahorse technology, we challenged the mitochondria to gain insight into the oxidative capabilities in both cell types as this could not be performed *in-vivo*. We investigated basal oxidative phosphorylation, basal glycolysis, mitochondrial respiration, ATP synthesis, spare respiratory capacity, non electron transport chain respiration and proton leak in both QH and OE33 cell lines. We demonstrate that metaplastic cells are more energy demanding compared with oesophageal cancer cells suggesting an early metabolic advantage for differentiation, metastatic transformation and subsequent proliferation due to an increased capacity to generate ATP for anabolic purposes.

When oxidative capacity of the QH and OE33 cells was challenged, mitochondrial respiration differed between the two cell types and the degree of ATP synthesis and proton leak attributed to mitochondrial respiration was also substantially different. The OE33 cell line maintains an equilibrium between both metabolic pathways thereby demonstrating metabolic plasticity while the QH cell line favours a more detrimental oxidative phenotype that may be selected during early stages of disease progression. Overall, we have shown in this study that metabolic reprogramming is active during disease progression in Barrett's and specifically, markers of oxidative phosphorylation can segregate Barrett's non progressors from progressors to cancer. This needs to be further examined using different patient cohorts from multicentres to establish clinical utility.

Conflict of interest

The authors declare no conflicts of interest.

Acknowledgements

The authors would kindly wish to acknowledge Dr. Richard Porter in the Department of Biochemistry, Trinity College Dublin, for access to the Seahorse XF24 flux analyser, Dr. Shane Duggan in the Department of Clinical Medicine, Trinity College Dublin (IMM), for all cell lines utilised throughout this study and Science Foundation Ireland for funding this research (SFI 11/RFP.1/CAN/3137). We would also like to thank the Oesophageal Cancer Fund (OCF) for supporting the biobanking of samples used in this study.

Appendix: Supplementary material

Supplementary data associated with this article can be found, in the online version, at doi:10.1016/j.canlet.2014.07.035.

References

[1] Z. Su, L.J. Gay, A. Strange, C. Palles, G. Band, D.C. Whiteman, et al., Common variants at the MHC locus and at chromosome 16q24.1 predispose to Barrett's esophagus, Nat. Genet. 44 (2012) 1131–1136.
[2] F. Hvid-Jensen, L. Pedersen, A.M. Drewes, H.T. Sorensen, P. Funch-Jensen, Incidence of adenocarcinoma among patients with Barrett's esophagus, N. Engl. J. Med. 365 (2011) 1375–1383.
[3] J. Ronkainen, P. Aro, T. Storskrubb, S.E. Johansson, T. Lind, E. Bolling-Sternevald, et al., Prevalence of Barrett's esophagus in the general population: an endoscopic study, Gastroenterology 129 (2005) 1825–1831.
[4] J. Jankowski, H. Barr, K. Wang, B. Delaney, Diagnosis and management of Barrett's oesophagus, BMJ 341 (2010) c4551.
[5] J.V. Reynolds, C.L. Donohoe, E. McGillycuddy, N. Ravi, D. O'Toole, K. O'Byrne, et al., Evolving progress in oncologic and operative outcomes for esophageal and junctional cancer: lessons from the experience of a high-volume center, J. Thorac. Cardiovasc. Surg. 143 (2012) 1130–1137.e1.
[6] V. Gogvadze, B. Zhivotovsky, S. Orrenius, The Warburg effect and mitochondrial stability in cancer cells, Mol. Aspects Med. 31 (2010) 60–74.
[7] A. Isidoro, M. Martinez, P.L. Fernandez, A.D. Ortega, G. Santamaria, M. Chamorro, et al., Alteration of the bioenergetic phenotype of mitochondria is a hallmark of breast, gastric, lung and oesophageal cancer, Biochem. J. 378 (2004) 17–20.
[8] K.G. Sifroni, C.R. Damiani, C. Stoffel, M.R. Cardoso, G.K. Ferreira, I.C. Jeremias, et al., Mitochondrial respiratory chain in the colonic mucosal of patients with ulcerative colitis, Mol. Cell. Biochem. 342 (2010) 111–115.
[9] J.M. Cuezva, M. Krajewska, M.L. de Heredia, S. Krajewski, G. Santamaria, H. Kim, et al., The bioenergetic signature of cancer: a marker of tumor progression, Cancer Res. 62 (2002) 6674–6681.
[10] R.A. Cairns, I.S. Harris, T.W. Mak, Regulation of cancer cell metabolism, Nat. Rev. Cancer 11 (2011) 85–95.
[11] F. Weinberg, N.S. Chandel, Mitochondrial metabolism and cancer, Ann. N. Y. Acad. Sci. 1177 (2009) 66–73.
[12] V. Fogal, A.D. Richardson, P.P. Karmali, I.E. Scheffler, J.W. Smith, E. Ruoslahti, Mitochondrial p32 protein is a critical regulator of tumor metabolism via maintenance of oxidative phosphorylation, Mol. Cell. Biol. 30 (2010) 1303–1318.
[13] N.G. Ericson, M. Kulawiec, M. Vermulst, K. Sheahan, J. O'Sullivan, J.J. Salk, et al., Decreased mitochondrial DNA mutagenesis in human colorectal cancer, PLoS Genet. 8 (2012) e1002689.
[14] D.A. Tennant, R.V. Duran, E. Gottlieb, Targeting metabolic transformation for cancer therapy, Nat. Rev. Cancer 10 (2010) 267–277.
[15] L. De Meirleir, S. Seneca, W. Lissens, I. De Clercq, F. Eyskens, E. Gerlo, et al., Respiratory chain complex V deficiency due to a mutation in the assembly gene ATP12, J. Med. Genet. 41 (2004) 120–124.
[16] D. Streif, E. Iglseder, C. Hauser-Kronberger, K.G. Fink, M. Jakab, M. Ritter, Expression of the non-gastric H+/K+ ATPase ATP12A in normal and pathological human prostate tissue, Cell. Physiol. Biochem. 28 (2011) 1287–1294.
[17] M. Huttemann, I. Lee, X. Gao, P. Pecina, A. Pecinova, J. Liu, et al., Cytochrome c oxidase subunit 4 isoform 2-knockout mice show reduced enzyme activity, airway hyporeactivity, and lung pathology, FASEB J. 26 (2012) 3916–3930.
[18] A. Baracca, F. Chiaradonna, G. Sgarbi, G. Solaini, L. Alberghina, G. Lenaz, Mitochondrial Complex I decrease is responsible for bioenergetic dysfunction in K-ras transformed cells, Biochim. Biophys. Acta 1797 (2010) 314–323.
[19] N. Bellance, G. Benard, F. Furt, H. Begueret, K. Smolkova, E. Passerieux, et al., Bioenergetics of lung tumors: alteration of mitochondrial biogenesis and respiratory capacity, Int. J. Biochem. Cell Biol. 41 (2009) 2566–2577.
[20] E. Bonora, A.M. Porcelli, G. Gasparre, A. Biondi, A. Ghelli, V. Carelli, et al., Defective oxidative phosphorylation in thyroid oncocytic carcinoma is associated with pathogenic mitochondrial DNA mutations affecting complexes I and III, Cancer Res. 66 (2006) 6087–6096.
[21] H. Simonnet, N. Alazard, K. Pfeiffer, C. Gallou, C. Beroud, J. Demont, et al., Low mitochondrial respiratory chain content correlates with tumor aggressiveness in renal cell carcinoma, Carcinogenesis 23 (2002) 759–768.
[22] H. Simonnet, J. Demont, K. Pfeiffer, L. Guenaneche, R. Bouvier, U. Brandt, et al., Mitochondrial complex I is deficient in renal oncocytomas, Carcinogenesis 24 (2003) 1461–1466.
[23] E.K. Hudson, B.A. Hogue, N.C. Souza-Pinto, D.L. Croteau, R.M. Anson, V.A. Bohr, et al., Age-associated change in mitochondrial DNA damage, Free Radic. Res. 29 (1998) 573–579.
[24] A. Isidoro, E. Casado, A. Redondo, P. Acebo, E. Espinosa, A.M. Alonso, et al., Breast carcinomas fulfill the Warburg hypothesis and provide metabolic markers of cancer prognosis, Carcinogenesis 26 (2005) 2095–2104.
[25] A.D. Ortega, M. Sanchez-Arago, D. Giner-Sanchez, L. Sanchez-Cenizo, I. Willers, J.M. Cuezva, Glucose avidity of carcinomas, Cancer Lett. 276 (2009) 125–135.
[26] D. Whitaker-Menezes, U.E. Martinez-Outschoorn, N. Flomenberg, R.C. Birbe, A.K. Witkiewicz, A. Howell, et al., Hyperactivation of oxidative mitochondrial metabolism in epithelial cancer cells in situ: visualizing the therapeutic effects of metformin in tumor tissue, Cell Cycle 10 (2011) 4047–4064.
[27] P.A. Cornford, A.R. Dodson, K.F. Parsons, A.D. Desmond, A. Woolfenden, M. Fordham, et al., Heat shock protein expression independently predicts clinical outcome in prostate cancer, Cancer Res. 60 (2000) 7099–7105.
[28] W. Ruan, Y. Wang, Y. Ma, X. Xing, J. Lin, J. Cui, et al., HSP60, a protein downregulated by IGFBP7 in colorectal carcinoma, J. Exp. Clin. Cancer Res. 29 (2010) 41.
[29] X. Thomas, L. Campos, C. Mounier, J. Cornillon, P. Flandrin, Q.H. Le, et al., Expression of heat-shock proteins is associated with major adverse prognostic factors in acute myeloid leukemia, Leuk. Res. 29 (2005) 1049–1058.
[30] J. Liu, L.D. Wang, Y.B. Sun, E.M. Li, L.Y. Xu, Y.P. Zhang, et al., Deciphering the signature of selective constraints on cancerous mitochondrial genome, Mol. Biol. Evol. 29 (2012) 1255–1261.
[31] F. Yao, T. Zhao, C. Zhong, J. Zhu, H. Zhao, LDHA is necessary for the tumorigenicity of esophageal squamous cell carcinoma, Tumour Biol. 34 (2013) 25–31.
[32] K. Koss, R.F. Harrison, J. Gregory, S.J. Darnton, M.R. Anderson, J.A. Jankowski, The metabolic marker tumour pyruvate kinase type M2 (tumour M2-PK) shows increased expression along the metaplasia-dysplasia-adenocarcinoma sequence in Barrett's oesophagus, J. Clin. Pathol. 57 (2004) 1156–1159.